*Journal of Applied Electrochemistry* **31**: 823–832, 2001.
© 2001 *Kluwer Academic Publishers. Printed in the Netherlands.*


# Electrochemical and gas evolution characteristics of direct methanol fuel cells with stainless steel mesh flow beds

K. SCOTT, P. ARGYROPOULOS, P. YIANNOPOULOS and W.M. TAAMA
*Chemical and Process Engineering Department, University of Newcastle upon Tyne, Merz Court, Newcastle upon Tyne, NE1 7RU, Great Britain*

Received 15 October 1999; accepted in revised form 1 February 2001

*Key words:* bipolar plates, carbon dioxide, direct methanol fuel cell, flow beds, gas bubbles, stainless steel

**Abstract**

Carbon dioxide gas management and bipolar plate (flow bed) design are important to the development of direct methanol fuel cell (DMFC) systems. If the gas produced at the anode is not removed rapidly and efficiently a gradual deterioration in electrical performance can occur. This paper examines the feasibility of using stainless steel mesh materials as flow beds for the DMFC. A flow visualization study, using a high-speed video camera and appropriate computer software, of the anode side, carbon dioxide gas evolution and flow behaviour with flow beds based on stainless steel mesh is reported. The electrochemical behaviour of the direct methanol fuel cell with stainless steel flow beds is also reported. A number of the flow bed designs, based on stainless steel mesh, showed promising behaviour in terms of gas removal characteristics and electrical performance.

## 1. Introduction

At present certain types of fuel cells (e.g., those based on solid polymer electrolyte) are commercially viable power sources for portable and transportation applications. Hydrogen fuel cells are more advanced and are now in the prototype-testing phase. However, the presence of a large, relatively heavy catalytic reformer poses one of the major obstacles to full commercialization of the technology. As a result of the problems associated with hydrogen based systems, the direct methanol fuel cell (DMFC), shown schematically in Figure 1, has recently received greater attention [1–9], which has resulted in a continuous improvement in electrochemical performance and in components for the cell.

The DMFC has long being considered to be the more difficult fuel cell technology due to two main reasons: (i) methanol crossover, through the polymer electrolyte membrane, to the cathode where methanol is oxidized. This results in a mixed cathode potential which lowers the cell performance and reduces fuel efficiency; and (ii) the lack of a cheap and highly efficient electrocatalyst for methanol oxidation. In addition, as cell-development work continues the engineering of the system has been largely neglected since commercialization of the relevant technology is still far away. Nevertheless, as experience with hydrogen based systems has shown, the engineering of the system should be considered in parallel with cell technology development to provide valuable feedback to cell designers and to minimize cost and potential manufacturing problems. A major issue for large cells and stacks is the flow bed design and fabrication material. The flow bed is responsible for reactants/products distribution to the membrane electrode assembly (MEA), and can be made in various ways (e.g., machining, pressing, injection moulding) [10].

A common flow bed material is 'nonporous' graphite but, due to problems associated with graphite, such as limited mechanical strength and microporosity, mixtures of thermoplastics (polyethylene, PVDF) or synthetic resins (phenolic, epoxy) with various types of carbon have been identified as promising candidates [11, 12]. Attempts have been made to reduce the cost and increase the long-term stability of the fuel cell plates [11–14] by the following methods:

(i) Simplification of the graphite flow bed design, thus reduce machining costs.
(ii) Replacement of graphite with a metal (e.g., stainless steel) and thus form the flow bed by, for example, etching.
(iii) Production of plates by moulding using, for example, conductive carbonaceous filler in a thermoplastic matrix.
(iv) Application of protective conductive coatings to the metal surface.

Nevertheless, in the potentially corrosive environment of an operating fuel cell the possibility of the formation of a passivating, film on the metal surface was considered an obstacle to progress in this area. Shukla [15] has recently reported data from a small scale DMFC stack that used a stainless steel flow bed, but did not disclose the exact material used. Although the performance

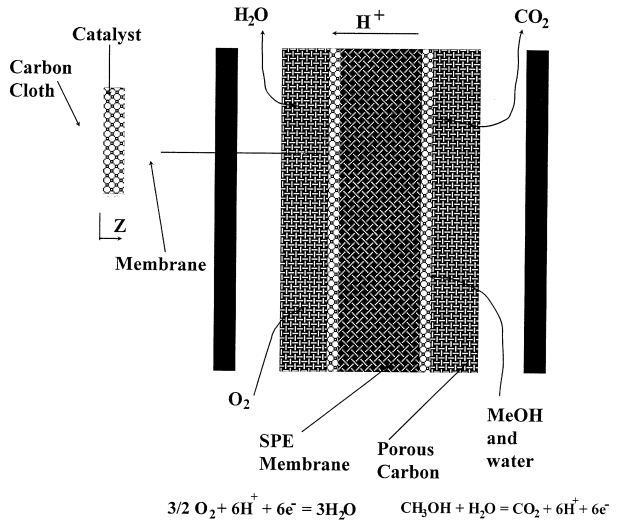


*Fig. 1.* Schematic diagram of the DMFC.

reported by Shukla was comparable with that achieved with similar graphite based cells, these were for very short-term studies, of a few hours. Davies et al. [16] examined alternative stainless steel materials for flow beds in hydrogen fuel cells. The study identified S316 and S310 stainless steels as promising in terms of performance and durability. Others have also used stainless steel based flow beds for hydrogen fuel cells [17, 18].

The efficient removal of carbon dioxide from the anode layer is a factor in the successful design and operation of the DMFC and depends significantly on flow bed and manifold design. The presence of relatively large amounts of carbon dioxide reduces the free area for the flow and penetration of reactants to the catalyst layer. This last phenomenon is affected by a high gas residence time in the cell, whereby the gas is trapped inside the gas diffusion layer and blocks the microchannels in that structure. This impedes the flow of methanol reactant to the anode catalyst and can cause concentration polarisation. Recently Arico et al. [13] investigated the effect of flow bed design on the electrochemical performance of a vapour fed DMFC. Their findings suggested that altering the flow bed design could affect the mass transfer characteristics of the vapour-fed DMFC and result in performance improvements and reduced methanol crossover. We have reported on the performance of the liquid-feed DMFC using two types of flow beds: a spot design and a parallel channel design [7]. The spot design electrical performance was superior to that of the parallel channel design at lower current densities (below 150 mA $cm^{-2}$) and was attributed to better gas management.

The present communication describes research carried out to assess the feasibility of using stainless steel flow beds in a small-scale DMFC. The electrochemical performance and the gas management characteristics with flow beds based on a parallel channel and five different stainless steel mesh is reported.

## 2. Experimental procedures

The electrochemical performance studies were conducted in three cells: graphite, graphite with stainless steel mesh and stainless steel (Figure 2). The cross-sectional area of the MEA was 9 $cm^2$ for all cells used. The cathode side flow bed was made from Poco® graphite block. The designs can be described briefly as follows:

(i) *Parallel channel*. Ten parallel flow channels, 2 mm deep, 2 mm wide and 30 mm long. The width of the ribs, which formed the flow channels, was 1 mm (Figure 2(a)).

(ii) *Spot*. Eight parallel series of spots, 2.0 mm deep, 1.5 mm wide, 1.5 mm long. The gap between two adjacent spots was 2.0 mm (Figure 2(b)).

(iii) *Mesh based*. A square shaped void of cross section 9.0 $cm^2$ and 2.0 mm deep with a groove of 1 mm width machined at the periphery. Three vertical ribs acted as support for the stainless steel mesh (Figure 2(c)). The assembly of the stainless steel mesh is shown in Figure 2(d).

For the flow visualization studies the anode side flow bed was made from acrylic.

Flow through the flow bed was via a two series of 2 mm diameter holes at the cell inlet and outlet, which connected into a 10 mm diameter ID internal manifold (Figure 2). Five different stainless steel mesh, supplied by Expamet, were used for this study with codes: 927S (Spec. 316/S31), 926S and 707S (Spec 304/S15) and Minimeshes (codes 941MM and 957MM) (Table 1). Each mesh had different geometric characteristics of porosity, thickness, openings and shape that enabled some assessment of the parameters that affect gas evolution behaviour.

In operation the cells were tested in a simple flow circuit, shown schematically in Figure 3, with methanol solution supplied, from a 2.5 $dm^3$ volume glass reservoir, by a Watson Marlow 505U peristaltic pump. Cell temperature was controlled using two electric heating plates (250 W) positioned against the cell retaining end plates. The temperature of the anode side solution was controlled by immersing the anolyte reservoir in a thermostatic controlled water bath. The anode side inlet and outlet fluid temperatures and the cell temperature were logged from a separate computer based data logger. Air was supplied from gas cylinders and the pressure was controlled by a needle valve at the cell cathode side outlet. The same experimental equipment was used for the electrochemical performance and flow visualization experiments. The methanol concentration was not monitored during the experiments as the relatively large reservoir ensured that the methanol concentration remained approximately constant for each set of experiments. This was confirmed by measurement of the concentration of the methanol before and after each set of experiments using an Abbe refractometer.

For the flow visualization studies the flows of methanol and carbon dioxide gas were recorded using a high

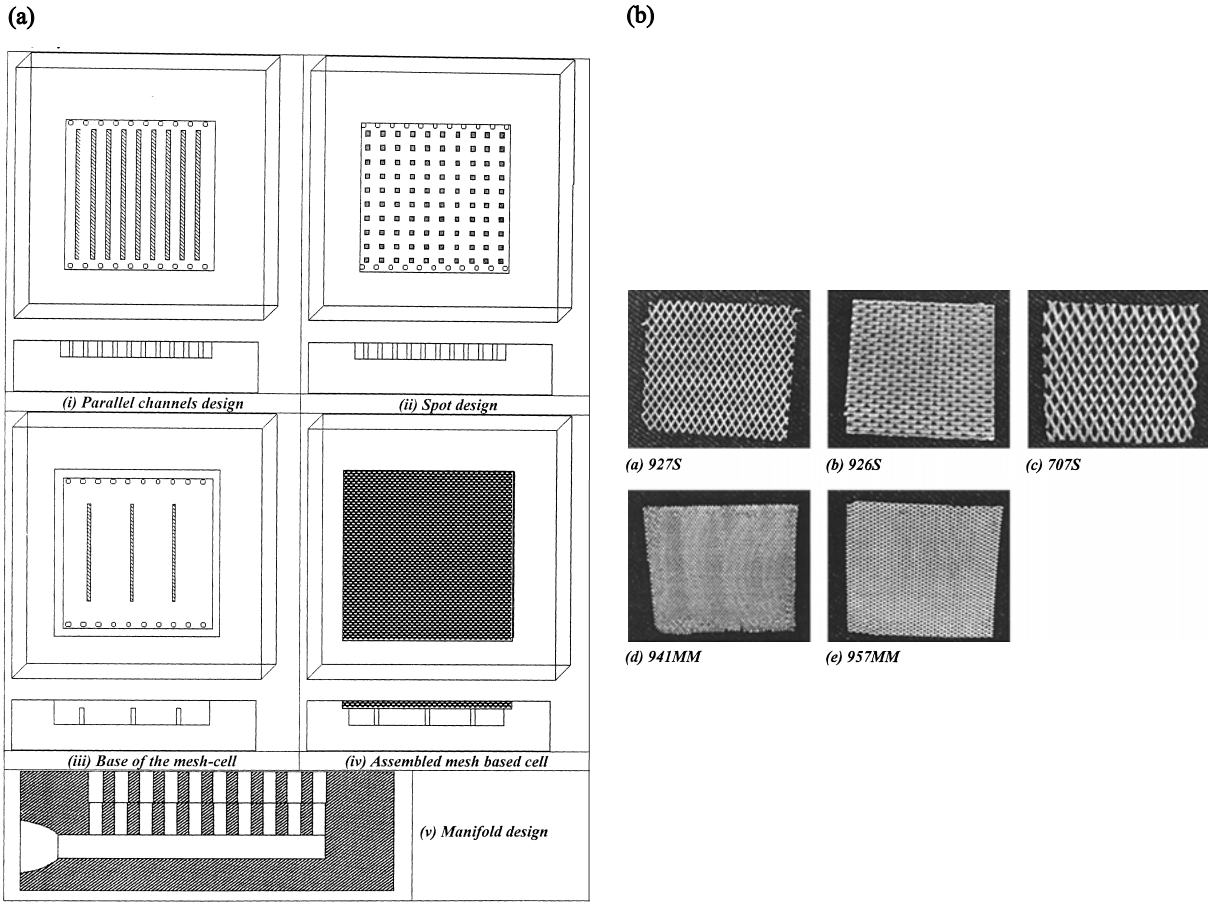


*Fig. 2.* Schematic diagram of the DMFC anode side flow beds and meshes. (a) Flow beds and (b) Stainless steel mesh. Codes as shown.

*Table 1.* Expamet mesh properties

| | 941MM | 957MM | 927S | 926S | 707S |
|---|---|---|---|---|---|
| Openings size /mm (LW) | 1 | 1.5 | 3.175 | 3.18 | 4.75 |
| Openings size /mm (SW) | 0.67 | 0.92 | 1.81 | 1.95 | 2.38 |
| Open area to total area /% | – | 46 | 60 | 12 | 43 |
| Strand width /mm | 0.2 | 0.22 | 0.254 | 0.79 | 0.56 |
| Size of strand thickness /mm | 0.15 | 0.15 | 0.152 | 0.46 | 0.46 |
| Weight per unit area /kg $m^{-2}$ | 0.8 | 0.62 | 0.34 | 2.91 | 1.69 |
| Measured thickness /$\mu$m | 204 | 220 | 220 | 1041 | 853 |

speed Hitachi CCTV video camera (HV-720K). A stroboscope was placed behind the camera to provide the necessary lighting for the camera. The images were stored directly in a computer unit with the aid of a Matrox PC card.

In this research two MEAs, produced by identical procedures, were used. One membrane electrode assembly was used for the flow visualization study and the second for the electrochemical performance study. Briefly, each MEA was fabricated as a sandwich of a solid polymer electrolyte membrane (Nafion® 117) between an anode and a cathode catalyst structure, which was hot-pressed at 100 kg $cm^{-2}$ for 3 min at 135 °C. Prior to fabricating the MEA, the membrane was pretreated by boiling for 1 h in 5 vol % $H_2O_2$ and then for 1 h in 1 mol $dm^{-3}$ $H_2SO_4$ and then washing in boiling Millipore water ( > 18 MΩ) for 2 h with regular changes of water. Electrode preparation procedures are described in detail elsewhere [7].

The anode consisted of a Teflonized (40%) carbon cloth support (E-Tek, type 'A'), 0.3 mm thickness, upon which was spread a thin (diffusion layer) layer of 10 wt % teflonized (ketjenblack 620) carbon. An anode catalyst layer was spread on the diffusion backing layer. The anode layer consisted of 40 wt % Pt–20 wt % Ru (2 mg $cm^{-2}$ total metal loading) dispersed on Vulcan XC72 carbon (E-TEK) and bound with 10 wt % Nafion®, from a 5 wt % Nafion® solution (Aldrich). In addition a thin layer of Nafion® solution was spread onto the surface of the catalyst layer to enhance proton conductivity between the catalyst layer and the solid polymer electrolyte membrane.

The cathode was constructed using a similar method as for the anode, using a thin diffusion layer bound with 10 wt % PTFE and a catalyst layer of 1 mg $cm^{-2}$ Pt black (Johnson Matthey) bound with 10 wt % Nafion®.

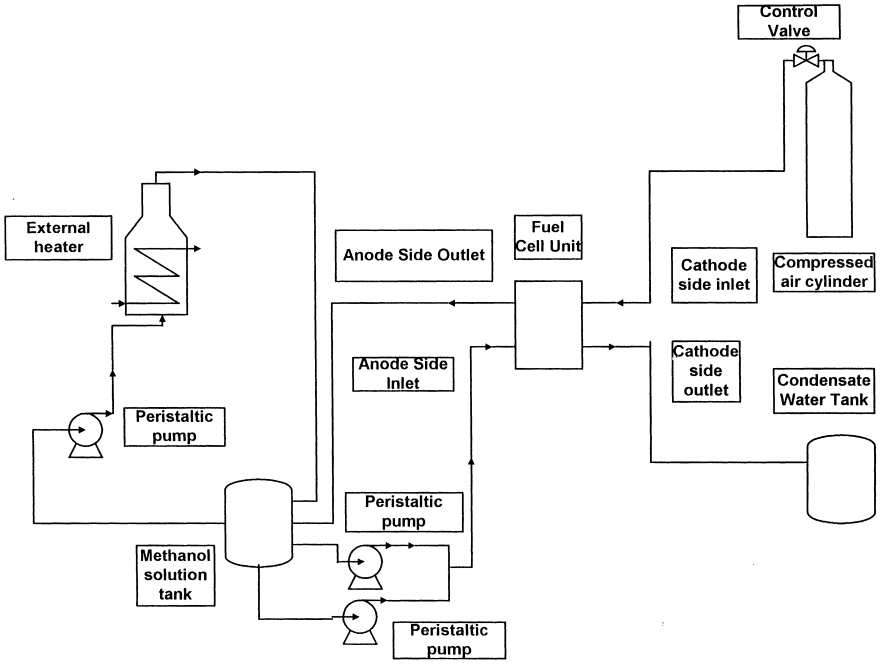


*Fig. 3.* Flow visualization experimental loop.

Due to the fact that each MEA was to be tested repeatedly in different cells the Teflon content of the carbon cloth was greater than usually used in fabrication (40% instead of 20%) [7], to make the cloth stiffer and more durable. This higher Teflon content resulted in a lower electrochemical performance than usually achieved and previously reported [7], but ensured consistent performance of the MEA during repeated use. The first tests of each MEA were performed in the parallel channel graphite cell to ensure reasonable performance of the MEA for the purposes of this programme. The series of tests were then conducted, twice, for each cell flow bed design. The MEA was then retested in the graphite flow bed cell to ensure consistency of performance. Cell voltage vs. current density response was measured galvanostatically, by incrementally increasing the current from open circuit and measuring the cell potential until a steady state was reached and then reducing the current incrementally, again measuring the cell voltage. The MEAs was conditioned before use in two stages: for 48 h in the test cell, in 2.0 mol $dm^{-3}$ methanol solution at 75 °C, and then by maintaining the cell with an applied load of 100 mA $cm^{-2}$ for several hours. This pretreatment resulted in stable performance under continuous operation.

## 3. Role of anode side flow bed design on cell operation

Within a working DMFC environment carbon dioxide, formed in the anode side electrocatalyst layer, flows counter to the aqueous methanol solution through the anode side gas diffusion layer and is released from the surface of the carbon cloth into the fluid flowing in the flow bed channels. In previous research we reported that gas management problems occur in small cells based on the design shown in Figure 1(a) [19, 20]. The surface morphology and characteristics of the gas diffusion-backing layer and the operating conditions of the cell were found to be important for bubble formation and removal. Toray carbon paper was found to give inferior gas removal properties in comparison to Type 'A' ETEK carbon cloth. This was explained from the texture of the paper surface (rough) and the resultant different surface tension and the enhanced friction between the bubbles and the material itself.

First, it was decided to consider (with the aid of a flow visualization study) the gas flow characteristics of the spot flow bed (Figure 1(b)) as part of the wides investigation of new flow bed designs. This was to assess if lowering the contact area available for friction will change the gas release and removal behaviour of the cell. The flow bed voidages were, 74% for the parallel channel design and 89% for the spot design. With the spot cell design there was no visual sign of large gas slugs, at least to the extent that significantly blocked the gas diffusion layer. More specifically, large gas bubbles were also formed (as was the case with the parallel channel design [19, 20]) but these bubbles were not stationary. Secondly, the bubbles did not block the entire channel cross section, as was the case in our previous studies [19, 20], ensuring an improved reactant supply to the catalyst layer.

The findings from the flow visualization study of the spot-based flow bed design indicated that there is a critical role for friction, between the 'walls' of the flow bed and the carbon dioxide bubbles, in gas accumulation. A requirement for a lower friction area contravenes the requirement for good contact area, between the block and the cloth surface, for effective current

collection and to minimize current distribution problems. This factor is particularly significant as the in-plane conductivity of the carbon cloth diffusion layer is much lower than the through plane conductivity which means that current should be collected close to its generation point otherwise significant power is lost to overcome this resistance. The combination of these factors lead to the inferior performance, at high current densities, of the cells with a spot based flow bed design [7, 9]. Furthermore, increasing the flow bed voidage reduces the mechanical support for the membrane electrode assembly. A requirement for low cost, high volume production adds to the problem of selection of a suitable flow bed design.

A potential design solution was therefore sought through the use of stainless steel mesh (Table 1). The moderate stainless steel conductivity is, to some extent, counteracted by the increase in contact area between the mesh and cloth. Hence, a combined flow visualization and electrochemical performance study was conducted to evaluate the effect of different types of mesh as flow beds for the DMFC.

## 4. Electrochemical and power performance of stainless steel mesh-based flow beds

Figure 4 compares the performance of the five different mesh based cells with that of the graphite cell, for the following operating conditions: 90 °C liquid temperature, 1 mol $dm^{-3}$ (M) solution concentration, 1.0 bar air pressure and anode side flow rate 500 $cm^3$ $min^{-1}$. The cell in these experiments was not directly heated by the heating plates but only by the use of the methanol solution at 90 °C. The cells using the 926S and 707S mesh based flow beds gave the best electrical and power performance, which is superior to that of the graphite based cell. At higher current densities the 707S mesh gave a slightly higher power density performance than the 926S mesh, which may be due to better gas management characteristics and mass transport combined with it lower thickness (approximately 300 $\mu$m less than the 926S mesh). The three cells based on the remaining mesh flow beds gave relatively poor performance, not achieving a power output at current densities above 100 mA $cm^{-2}$. As can be seen in Figure 4 the 927S mesh gave the poorest electrical performance, 941S gave the second poorest, and finally 957MM gave the third poorest performance.

The performance of the fuel cell is clearly influenced by the type and geometry of the mesh used (Table 1). The two meshes that gave superior performance, compared with the graphite cell, are the thickest. The 926S mesh has a smaller open area, combined with a large strand width and thickness. The 707S had a large width of strand and the second smallest open area. The remaining three mesh were much thinner and more flexible than either the 926S or 707S mesh and had a greater open area. These combined characteristics indicate that the 927S, 957S and 941S mesh do not have an efficient current collection facility, from the MEA, in comparison to the 926S and 707S mesh. In addition the type of mesh would also be expected to influence the flow distribution and gas evolution characteristics and thus a flow visualization study was undertaken to investigate the gas management properties of the new structures.

The effect of cathode side air pressure (0.5 to 2.0 bar) on the performance of the cells with the 927S and 707S mesh is shown in Figure 5. There is a modest improve-

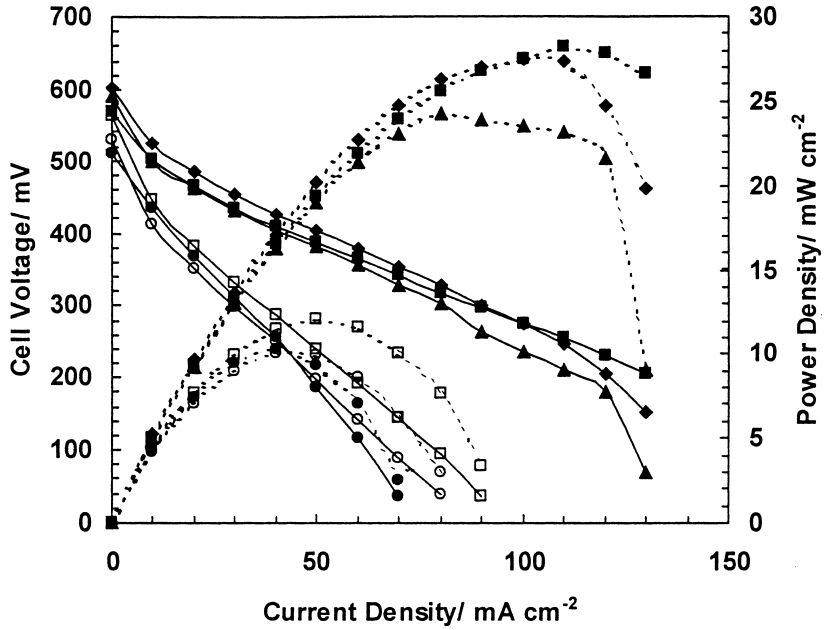


*Fig. 4.* Comparison of the polarization and power density data for the DMFC with six different flow beds. Liquid temperature 90 °C, 1.0 M methanol, 1 bar air, anode side flow rate 500 $cm^3$ $min^{-1}$. Key: (◆) 926S, (●) 927S, (■) 707S, (□) Poco®, (○) 957MM, (□) 941MM.

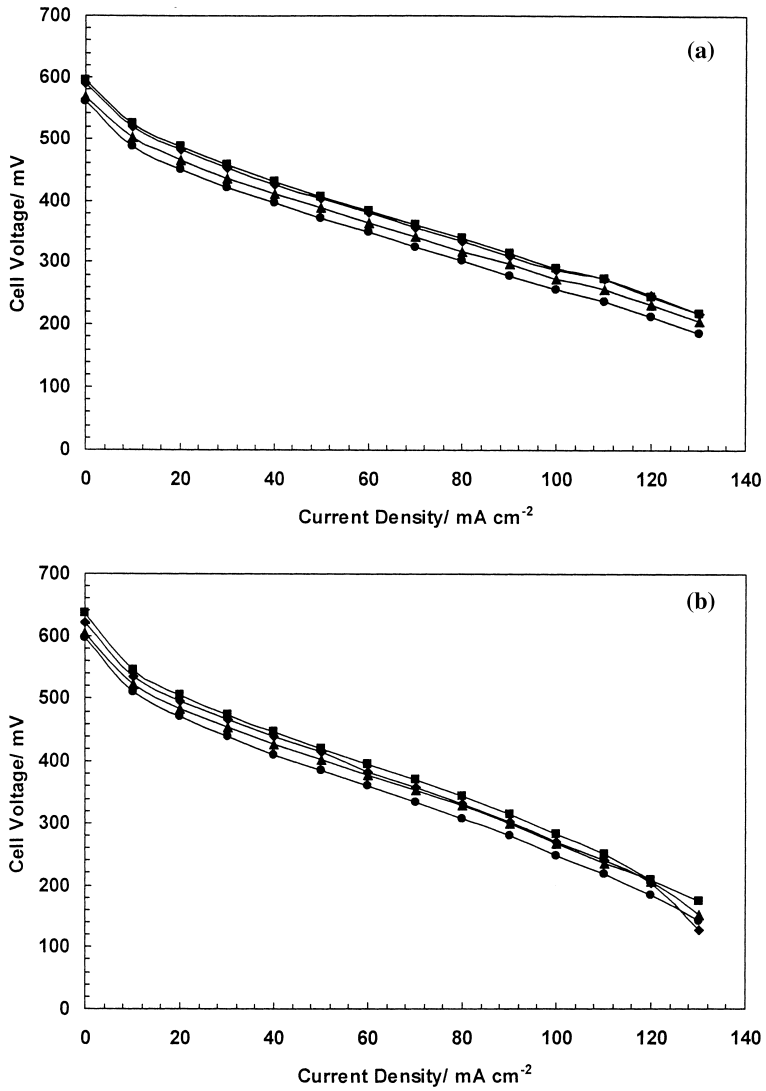


*Fig. 5.* Effect of cathode air pressure on the performance of the DMFC with 926S and 707S stainless steel mesh. Liquid temperature 90 °C, 1.0 M methanol, anode side flow rate 500 $cm^3$ $min^{-1}$. Key: (●) 0.5 bar, (▲) 1.0 bar, (◆) 1.5 bar, (■) 2.0 bar. (a) 926S mesh and (b) 707S mesh.

ment in performance with increasing pressure in line with previously obtained [7] with the graphite flow bed. This data does not indicate that there are particular problems with poor contact resistance between the mesh and MEA when lower air pressures are applied. The behaviour of the cells over a range of anode side flow rates (50–500 $cm^3$ $min^{-1}$) was similar to that shown in Figure 4.

The electrical performance of the five mesh based flow bed cells can be summarized in the following order (from the best to the worst):

$$707S \Rightarrow 926S \Rightarrow 957MM \Rightarrow 941MM \Rightarrow 927S$$

## 5. Gas management characteristics of stainless steel mesh-based flow beds

Figure 6 shows snapshots, taken from high speed video recordings, of the gas evolution at the anode side of the five, mesh based, DMFCs operating at an anode side flow rate of 5 $cm^3$ $min^{-1}$ and at two current densities (10 and 220 mA $cm^{-2}$). A few general comments are necessary to assist in distinguishing the bubble release from the surface; in every frame there are three strips, lighter in tone than the remaining area, that are essentially the three acrylic ribs supporting the mesh. Light grey areas in the dark background show bubbles, either accumulating or flowing with the liquid flow. In general, in all frames, the gas accumulation was in the form of small bubbles or bubble swarms flowing in the flow bed structure. This is in contrast with the behaviour of the parallel channel design where significant gas accumulation was experienced and flow channels became blocked by gas [19, 20]. Further details of the gas evolution characteristics at different operating conditions can be found in reference [21]. We summarise hear the observed gas evolution characteristics of the mesh based cells:

The 927S mesh had a relatively thin open structure with lozenge shaped openings and showed a tendency to trap carbon dioxide bubbles within its structure (Figure 6). Even with a relatively large anode side flow

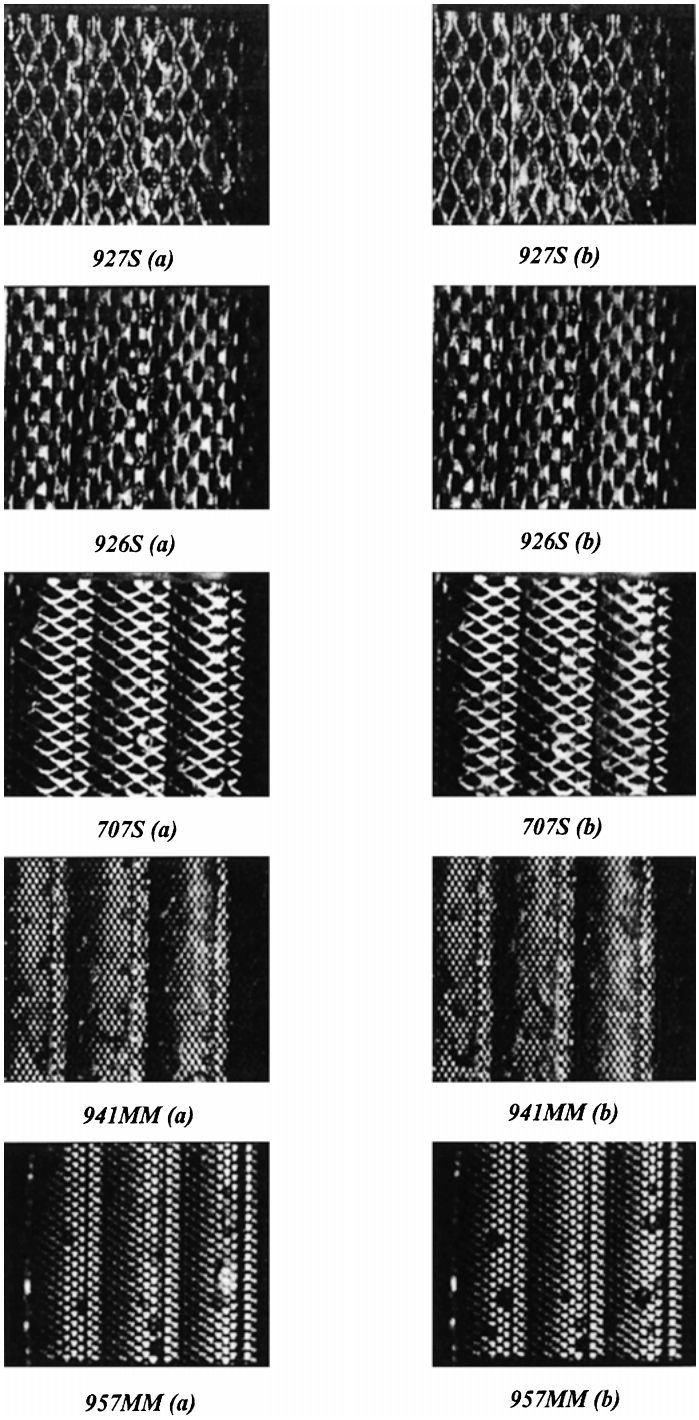


*Fig. 6.* Gas evolution behaviour of the anode side of the DMFC with mesh based flow beds. Methanol solution inlet flow rate 5 $cm^3$ $min^{-1}$, 2.0 bar cathode air pressure, 2.0 M methanol solution, liquid inlet temperature 80 °C. Mesh codes as shown. Current density: (a) 10 and (b) 220 mA $cm^{-2}$.

rate (500 $cm^3$ $min^{-1}$) there were still a number of bubbles trapped in the mesh structure. Overall this mesh gave the poorest gas management behaviour of all five meshes.

The 926S mesh was thick, with a dense structure (i.e., low open area to total area ratio) and triangle shaped openings. Despite the reduced number of openings per unit area this mesh showed no gas accumulation even when operated at 220 mA $cm^{-2}$ and a relatively low anode side flow rate (5.0 $cm^3$ $min^{-1}$). Over the duration of the experiments the study showed that the gas was removed immediately after evolution from the gas diffusion layer in the form of fine, fast moving bubbles and practically no gas accumulation occurred in the cell.

The 707S mesh had a similar geometry, in terms of void area, to 927S and its thickness was comparable to 926S. The gas management was characterised by the formation of large gas bubbles that were not trapped in the mesh structure. Additionally, as was verified from experiments involving a constant increase in anode side

flow rate, there was a significant improvement in gas removal at higher current densities.

941MM and 957MM were 'minimesh' and are thin with a large number of small holes per unit area. The 941MM mesh was the finest and in operation bubbles tended to attach to the mesh surface. Experiments showed that, with a current density of 100 mA $cm^{-2}$, the use of an anode side flow rate in excess of 250 $cm^3$ $min^{-1}$ was necessary to achieve an acceptable level of gas removal from the cell. The 957MM mesh showed a slightly better gas evolution behaviour than the 941MM mesh, i.e. a lower tendency for bubble accumulation on its surface.

Overall the five meshes examined can be classified according to their gas management characteristics, that is, the lack of bubble accumulation in the structure, in the following order (from the best to the worst):

$$926S \Rightarrow 707S \Rightarrow 957MM \Rightarrow 941MM \Rightarrow 927S$$

In general the cells with a mesh based flow bed showed superior gas management in comparison with designs based on parallel channels and spots.

From the present study two parameters were identified as significant in terms of gas accumulation within the cell: mesh thickness and voidage. Minimesh and thin mesh, with an open structure, do not appear to be suitable materials. It seems that an effective mesh may act as a 'bubble breaker', that is, as the gas is evolved it is forced to pass through a relatively thick, dense structure that breaks the bubbles into smaller size. In addition the surface of the minimesh was quite smooth, which would not help in bubble detachment. On the contrary the surfaces of 926S or 707S were relatively rough and there was no indication of slug formation or bubble attachment.

Generally the mesh would help create local turbulence, which enhances mass transfer characteristics between the cloth surface and the aqueous methanol solution. Furthermore, increased turbulence leads to enhanced heat transfer between the membrane electrode assembly and the anode side preheated liquid. Finally, the presence of the mesh may also improve current distribution.

Overall, in the experiments conducted with 926S and 707S mesh, the peak power performance improvement was between 5–15% compared with the graphite flow bed. This is a preliminary investigation with five different mesh chosen from one manufacturers product line and one MEA structure. Although the use of stainless steel mesh as a flow bed shows potential, at least from the points of view of gas management and cost, the change in the cell resistance and the potential improvement in the current distribution and the cell's mass transfer characteristics should also be assessed. Further studies are required to fully assess the potential of using mesh in a DMFC.

## 5. Stainless steel flow beds

Davies et al. [16] examined alternative types of stainless steel materials for flow beds in hydrogen fuel cells. The study identified S316 and S310 stainless steels as promising in terms of performance and durability. For the current work a stainless steel (S316) parallel channel flow bed was used to test the long term performance. The cell was operated in the combined preheated feed and cell mode. Figure 7 shows the voltage output and the power density of the cell over a range of methanol solution flow rates. The cell was heated at 70 °C using a 1.0 M aqueous methanol solution supplied at 85 °C and air supplied at a pressure of 2 bar. As can be seen, from

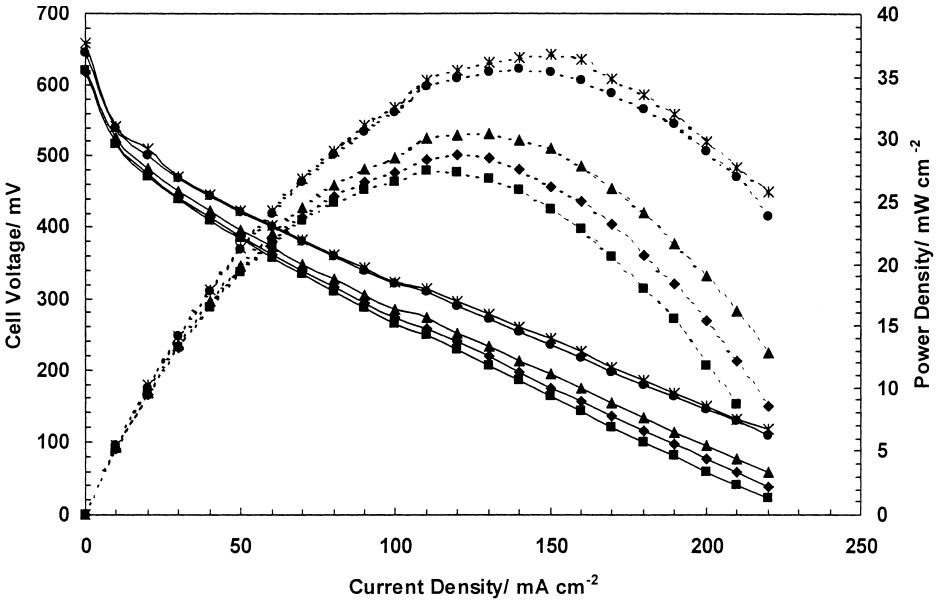


*Fig. 7.* Effect of anode side flow rate on the voltage and power density performance of the DMFC with a stainless steel, S316, parallel channel flow bed. Key: (■) 5.0, (◆) 25.0, (▲) 50.0, (●) 250.0 and (*) 500.0 $cm^3$ $min^{-1}$.

Figure 7, the voltage and power response increased with increasing flow rate. This was because, as the flow rate was increased, the improved heat transfer increased the anode catalyst layer temperature (i.e., the feed temperature is higher than the cell block temperature), and thus enhanced the methanol oxidation kinetics, and also improved the gas removal characteristics.

Figure 8 shows the effect of cathode side pressure on the voltage response and the power performance of the stainless steel cell. As can be seen, the cell response was improved with a higher air pressure and the data was similar to that obtained previously with a graphite cell [7, 9]. In general the stainless steel cell gave a comparable performance with that achieved with the graphite cell with the same flow bed design ([7, 9]). Up till now the stainless steel DMFC has been operated for six months (polarisation data collected approximately on a weekly basis) with no appreciable performance loss (Figure 9). Monthly visual inspections have shown no discolouration or other evidence of corrosion or passivating films.

## 6. Conclusions

A flow visualization study, with an acrylic DMFC, has been used to help understanding the effect of flow bed geometry on carbon dioxide evolution and removal from the anode side flow bed. The study investigated a series of stainless steel mesh as an alternative flow bed design. The

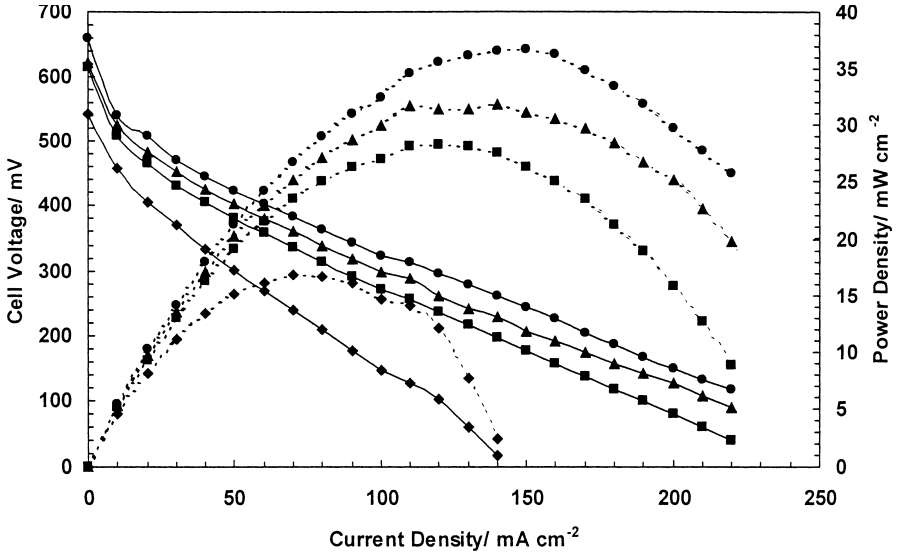


*Fig. 8.* Effect of cathode side air pressure on the voltage and power density performance of a DMFC based on stainless steel (S316) parallel channel flow bed. Pressure: (◆) 0, (■) 1.0, (▲) 1.5 and (●) 2.0 bar.

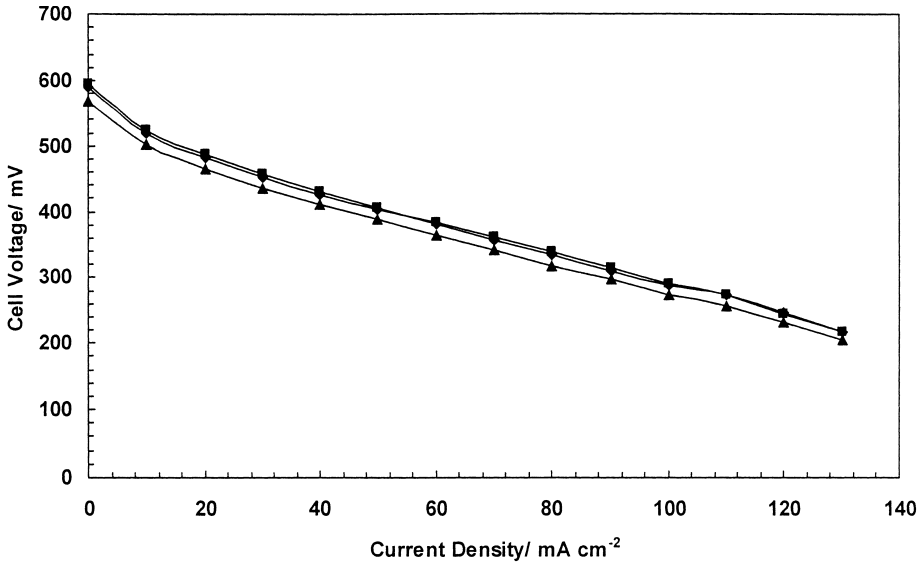


*Fig. 9.* Effect of extended operation on DMFC performance. Methanol solution inlet flow rate 5 cm$^3$ min$^{-1}$, 0.5 bar cathode air pressure, 2.0 M methanol solution. Liquid inlet temperature 80 °C. Period: (■) 5, (▲) 15 and (●) 160 day.

study identified relatively thick mesh with low voidage and a 'rough' surface as promising candidate materials. Fine minimesh and open structured mesh gave relatively poor performance. Certain mesh exhibited good gas removal characteristics and realised improved performance in comparison to graphite cells with parallel flow channels. Improvements of 5–15% in peak power density were obtained for two mesh materials. Further research is required to characterise the electrochemical performance of these cells and to investigate a larger range of mesh to identify, and optimize, the most promising commercially available product.

Stainless steel flow beds have been tested successfully over prolonged time periods and gave comparable performance with that of graphite cells. Further performance improvements are expected with new cell designs that capitalise on the mechanical and electrical properties of stainless steel.

## Acknowledgements

The authors would like to acknowledge the EPSRC for financial support and The European Commission for a TMR Marie Curie B20 research training grant to P.A.

## References

1. X. Ren, S.C. Thomas, P. Zelenay and S. Gottesfeld, 1998 Fuel Cell Seminar, Palm Springs, CA (1998).
2. X. Ren, M.S. Wilson and S. Gottesfeld, *J. Electrochem. Soc.* **143** (1996) L12.
3. T.I. Valdez, S.R. Narayanan, H. Frank and W. Chun, Annual Battery Conference on Applications and Advances, Long Beach, USA (1997).
4. S.R. Narayanan, T. Valdez, N. Rohatgi, W. Chun and G. Halpert, *1998 Fuel Cell Seminar,* Palm Springs, CA (1998).
5. S.R. Narayanan, G. Halpert, W. Chun, B. Jeffries-Nakamura, T.I. Valdez, H. Frank and S. Surampudi, *Electrochemical Society Annual Meeting,* Los Angeles, CA (1996).
6. S.R. Narayanan, G. Halpert, W. Chun, B. Jeffries-Nakamura, T.I. Valdez, H. Frank and S. Surampudi. *37th Power Sources Conference*, Cherry Hill, NJ (1996).
7. K. Scott, W.M. Taama and P. Argyropoulos, *J. Appl. Electrochem.* **28** (1999) 1389.
8. K. Scott, W.M. Taama and P. Argyropoulos, *J. Membrane Science* **171** (2000) 119.
9. K. Scott, W.M. Taama and P. Argyropoulos, *J. Power Sources* **79** (1999) 43.
10. J. Scholta, B. Rohland, V. Trapp and U. Focken, *J. Power Sources* **84** (1999) 231.
11. D.N. Busick and M.S. Wilson, *1998 Fuel Cell Seminar,* Palm Springs, CA (1998).
12. K. Ledjeff-Hey, F. Mahlendorf, O. Niemzig and A. Trautmann, *1998 Fuel Cell Seminar,* Palm Springs, CA (1998).
13. A.S. Arico, P. Creti, V. Baglio, E. Modica and V. Antonucci, *Electrochimica Acta* **45** (2000) 4319.
14. G. Xie and H. Okazaki, *3rd International Fuel Cell Conference*, Nagoya, Japan (1999).
15. A.K. Shukla, M.K. Ravikumar, M. Neergat and K.S. Gandhi, *J. Appl. Electrochem.* **29** (1999) 129.
16. D.P. Davies, P.L. Adcock, M.T. Turpin and S.J. Rowen, *J. Appl. Electrochem.* **30** (1999) 101.
17. R. Hornungand, G. Kappelt, *J. Power Sources*, **72** (1998) 20.
18. K.B. Prater. *J. Power Sources* **61** (1996) 105.
19. P. Argyropoulos, K. Scott and W.M. Taama, *J. Appl. Electrochem.* **29** (1999) 661.
20. P. Argyropoulos, K. Scott and W.M. Taama, *Electrochim. Acta.* **44** (1999) 3575.
21. P. Argyropoulos, 'Performance and Modelling of the Direct Methanol Fuel Cell,' PhD thesis, University of Newcastle upon Tyne, UK (1999).